A Self-Consistent Charge-Embedding Methodology for ab Initio Quantum Chemical Cluster Modeling of Ionic Solids and Surfaces: Application to the (001) Surface of Hematite (α-Fe_2O_3)†

Enrique R. Batista and Richard A. Friesner*

Department of Chemistry and Environmental Molecular Sciences Institute, Columbia University, New York, New York 10027

Received: February 26, 2002; In Final Form: June 11, 2002

To ab initio simulate an ionic crystal using a cluster of atoms, one must surround that cluster with point charges. These point charges add the effect of the electrostatic potential of the rest of the crystal on the electronic structure of the quantum cluster. The value of the point charges has to be chosen to reproduce the crystal field in the region of the cluster. In this work, a method to compute the necessary point charges is presented. The algorithm to choose the point charges is an extension of the one presented by Derenzo et al. [*J. Chem. Phys*. **2000**, *112*, 2074]. The method consists of a self-consistent loop, fitting in each iteration the value of the point charges to reproduce the electrostatic field, calculated from the quantum simulation, in the region of the cluster. This method was then applied to the study of the (001) basal surface of hematite, α-Fe_2O_3. As the cluster size is systematically increased, it is shown that to fully converge the electrostatic effect on the electronic structure of the cluster, clusters of the order of 60 atoms are necessary. As a convergence parameter for the cluster to the bulk behavior, we used the ionization energy of the cluster. In the limit of an infinite cluster, we obtained the work function of hematite to be 5.6 eV.

1. Introduction

There are two fundamental approaches to modeling solid state systems via ab initio quantum chemical techniques. The first is to employ periodic boundary conditions on the Schroedinger equation, which naturally leads to the use of plane waves as the one particle basis set in a numerical implementation. Plane wave codes based on density functional theory (DFT) such as the Car−Parinello approach[1] or the VASP program of J. Hafner and co-workers[2] are now widely used to carry out materials simulations. The development of accurate and efficient pseudopotential methods,[3,4] along with gradient corrected DFT functionals,[5,6] has enabled these methods to achieve great success in studying a substantial range of chemical problems.

The second approach is to perform cluster calculations, extrapolating toward condensed phase results by a combination of increasing cluster size and the use of embedding methods (i.e., treatment of the region outside the quantum cluster via approximate representations, such as classical point charges). For the investigation of bulk solids, this approach is probably not competitive with plane wave techniques, which have the natural advantage of building the appropriate boundary conditions directly into the basis functions. However, for more complex structures—for example, structural defects in solids, molecules adsorbed on surfaces, or a liquid−solid interface—cluster methods have some potential advantages. First, one is not restricted to the use of gradient corrected DFT approaches but can employ hybrid functionals or even higher-level ab initio methods, which for some types of problems can provide greater accuracy. Second, if the structural defects or adsorbates are dilute, a cluster model may be a better physical representation. Third, for inhomogeneous systems, the issue of computational efficiency for a given level of accuracy is far from settled. The use of localized Gaussian orbitals allows an accurate treatment of highly localized metal d electrons at a relatively low cost, as well as the ability to treat rather large inhomogeneous structures (e.g., a large molecule adsorbed on a surface) easily. When combined with QM/MM-type embedding methods, the effects of the condensed phase environment can be robustly represented, provided that one is interested in local interactions as opposed to delocalized properties like band structure. Finally, these methods can be readily extended to address solid−liquid interfaces via a continuum dielectric treatment of the solvent, an approach that has yet to be adapted to plane wave based programs. Thus, there are good reasons to pursue the development of an efficient and accurate cluster-based approach to modeling surfaces and other complex solid-state structures.

In the present paper, we describe the use of cluster methods to treat ionic solids. For systems of this type, a quantum cluster is surrounded by classical ions whose charges are determined self-consistently by iterated calculations in the quantum region, carried out in the field of the classical ions. A key idea of the present paper is to ensure that the field generated by the surrounding classical ions is able to represent the electrostatic potential generated by ions in the infinite solid. This can be accomplished in relatively straightforward fashion by determining the classical potential using Ewald methods and then fitting a finite set of point charges to reproduce this potential in the relevant region of the calculation (i.e., in the region of the quantum part of the cluster). The details of this methodology are presented below.

To demonstrate the effectiveness of our approach, we apply the method to a challenging problem, modeling of the (001)

† Part of the special issue "John C. Tully Festschrift".

* Corresponding author. Address: 3000 Broadway, Department of Chemistry, MC-3110, Columbia University, New York, NY, 10027. E-mail: rich@chem.columbia.edu.

10.1021/jp020509b CCC: $22.00
Published on Web 07/16/2002

surface of hematite, a material which has important technological and environmental applications. We calculate the ionization potential of hematite and examine the effects of the embedding method, type of DFT functional used, basis set size, and cluster size and shape. Converged results are obtained which compare favorably with experimental estimates of ionization potential. Our results differ from those presented by Wang et al.,[7] who calculated the same quantity using plane wave DFT based methods, and are considerably closer to the experimental values at least based on the estimates that we are able to make. Further work will be required to identify the origin of this discrepancy and to determine which value is in best agreement with accurate determined experimental data (which is not yet available).

The paper is organized as follows. Section 2 describes the algorithm that we use for our embedding methodology. Section 3 discusses details of the hematite modeling, including construction of the structural model for the hematite surface, specifics of the embedding model for hematite, and treatment of the spin states of the iron atoms in the cluster. Section 4 presents results obtained for the ionization potential of hematite for a series of clusters of increasing size, demonstrating convergence as a function of surface area and perpendicular depth of the cluster. Section 5, the Conclusion, discusses the significance of the results as well as future directions.

2. Point Charges Approach

To study phenomena dependent on the local structure of a crystal, the natural approach is to approximate the crystal with a cluster of atoms. This finite cluster is set to reproduce the local structure of interest, crystal defects, adsorbed atoms or molecules, etc. The defect in this type of calculation is that it uses a finite cluster size, on the order of 10 Å on the side, and this leads to missing contributions from the rest of the crystal, namely, all the lattice atoms not included in the cluster. In ionic crystals the effect is clear because the coulomb field is a long-range interaction. The field of all the crystal charges has an effect in the region of the cluster. In a perfect crystalline array of point charges, the electrostatic potential at an arbitrary point can be written as a sum over the contributions from the charges just in a unit cell as

$$U(\vec{r}) = \sum_{\vec{n}} \sum_{i} \frac{q_i}{|\vec{r} - \vec{r}_i - \vec{n}|} \tag{1}$$

where q_i's are the charges in the unit cell, located at positions $\vec{r}_i$'s and the sum over $\vec{n} = (n_x a_x + n_y a_y + n_z a_z)$ is a sum over all the points of the orthorhombic lattice defined by the integer numbers (n_x, n_y, n_z) and the dimensions of the unit cell (a_x, a_y, a_z). We can rewrite the potential as

$$U(\vec{r}) = \sum_{i} \frac{q_i}{|\vec{r} - \vec{r}_i|} \sum_{\vec{n}} \frac{|\vec{r} - \vec{r}_i|}{|\vec{r} - \vec{r}_i - \vec{n}|} \tag{2}$$

$$= \sum_{i} \alpha(\vec{r} - \vec{r}_i) \frac{q_i}{|\vec{r} - \vec{r}_i|} \tag{3}$$

where $\alpha(\vec{r})$ is the Madelung constant

$$\alpha(\vec{r}) = \sum_{\vec{n}} \frac{|\vec{r}|}{|\vec{r} - \vec{n}|} \tag{4}$$

The sum of the Madelung constant is conditionally convergent. There is an extensive amount of work in the literature on how to calculate this sum.[8,9] To include this long-range effect in the calculation of the electronic structure of the cluster, surrounding the cluster with a large number of point charges is not enough. Truncating the sum of the electrostatic contributions can lead to serious errors coming from the truncated surface that do not necessarily diminish when the number of point charges is increased; one needs to include the full sum.

An alternative technique to using a complete Ewald summation consists of approximating the sum by embedding the cluster in a large number of point charges. Different spacial arrangements of point charges have been suggested in the literature to better reproduce the crystal potential. Stefanovich and Truong[10] place point charges on a surface surrounding their cluster. In their approach the point charges are fitted to reproduce the potential at that surface generated by the charges of the ionic crystal outside the surface. The number of points where the potential is sampled equals the number of unknown point charges. Two other suggested placements for the embedding charges consist of laying them at random in space or placing the embedding point charges at the crystalographyc lattice sites.[11] Derenzo et al.[12] found better fitting of the electrostatic potential in the region of the cluster using the last of the three approaches, which is also the arrangement adopted in this work. The algorithm to fit the embedding charges can be summarized as follows:

(i) Calculate the ionic crystal potential at a collection of sampling points in the region of the cluster and in its surroundings. This calculation has to be done using methods of the Ewald type[8,13] to calculate the infinite sum of the Madelung constant.

(ii) Separate the embedding charges in two regions: near embedding charges, charges within a certain distance of the cluster and far embedding charges, charges outside the near region and up to the edge of the embedding set of point charges.

(iii) Fit the far embedding charges to reproduce, as best as possible, the potential generated by the crystal point charges outside the near region, that is, the full series minus the potential from the near embedding charges.

Derenzo et al.[12] have shown that when the near and far regions are properly chosen, this method is very effective in reproducing the electrostatic potential field of an ionic crystal in the region of the cluster. Once the effect of the rest of the crystal is known, one can assume it to be constant and study the local changes in the structure by modifying the quantum region and introducing the effect of the rest of the crystal through the field of the point charges.

To use the embedding method to simulate the crystal environment, there still remains an additional decision to be made: The amount of charge to be assigned to each lattice site of the unit cell on step i of the algorithm described above. The simplest approach is to assign formal charges to the lattice sites, that is, the charge expected from the ionization state of the atom that would have occupied that lattice site.[14,15] However, such assignment can lead to serious problems of accuracy. To achieve more accurate results, the actual charge to be assigned should be the appropriate one necessary to reproduce the field from the rest of the crystal in the region of the quantum cluster, as that is what the point charges are modeling. When one is simulating a bulk environment and all the atoms of each type are in similar environments, one could expect that the net charges of the atoms will be proportional to the ionization state of the atom under consideration. This conclusion can be drawn from the conservation of the total charge of the system and by imposing the symmetry that all atoms of each type should have the same amount of charge. However, the constant of propor-

tionality remains an unknown quantity, and one should in principle fit this constant to agree with the charge distribution from the quantum part of the simulation. When the simulation involves open surfaces, the symmetry of the crystal is broken in the direction perpendicular to the surface, and one cannot assume that the atoms are in equivalent environments anymore; all the charges in the unit cell must then be allowed to vary and should be selected to generate a field consistent with a periodic array of the unit cells.

What follows is an algorithm extending the one presented by Derenzo et al.[12] to choose the charges necessary to more accurately embed a quantum cluster. The algorithm includes a protocol for adjustment of the point charges to agree with the quantum cluster. The embedding point charges were located at the lattice sites of the crystal. Three regions of the embedding charges should be distinguished: region 0, an extended unit cell of the crystal that contains the quantum cluster; region 1, embedding charges near the quantum cluster defined as the lattice points within a chosen distance, R_1, from any atom in the cluster; region 2, embedding charges far away from the cluster, defined as the lattice sites at a distances larger than R_1 and up to the cutoff radius, R_2, from any quantum atom. The algorithm is as follows:

(i) Make an initial guess for the embedding charges.

(i) Calculate the electronic structure of the cluster under the influence of the embedding charges.

(iii) Calculate the electrostatic potential at a collection of sampling points in the region of the cluster.

(iv) Use the charges in region 0 to fit the electrostatic potential calculated in step iii. For the potential produced by each charge in the unit cell, an Ewald-type function is used that takes into account the effect of the infinite periodic array of replicas. This has the effect of fitting an infinite array of point charges, placed at the crystal lattice sites. For two-dimensional surface simulations, we used a thick slab and the two-dimensional form of the potential derived by Lekner[16] for square cells, extended by Clark et al.[17] to rectangular cells.

(v) Using the unit cell charges fitted in step iv, calculate the electrostatic potential field at a collection of sampling points, not only in the region of the cluster but also in the surrounding near region, around the atoms in region 1. This field has to be calculated using the infinite periodic replicas of the unit cell.

(vi) After discounting the potential contribution from the near charges, fit the embedding charges in region 2 to reproduce the far field.

(vii) Using the new set of charges, return to step ii until convergence in the value of the point charges is observed.

This algorithm converges when the field generated by the periodic array of the point charges equals the field in the region of the quantum cluster. One should not overinterpret the physical meaning of the point charges used; they do not represent the charge of the atoms in the crystal. The point charges are just charges chosen to reproduce the field of the rest of the crystal in the region of the cluster by fitting the field of the infinite array with a finite number of point charges.

We should also note that using point charges to represent the ions is, in itself, an approximation. As such, this model will be more accurate the more ionic the crystal is. If the crystal were perfectly ionic, the assumption would be valid, but otherwise it should be taken as the first-order term in a multipole expansion of the charge density of the ions.

3. Application to the Simulation of the Basal Face of Hematite

The surface chemistry of iron oxide plays an important role in technological applications, such as catalysts in dehydrogenation reactions[18] or as magnetic devices.[19] Also, given the abundance of iron oxides on the earth's crust, the understanding of their surface chemistry is one of the key issues in the study of environmental problems such as the transport of organic material and heavy metals as they move through the soil. Therefore, it is very important to have a technique to study surface chemistry in these materials.

Computer simulations of the surface of iron oxide are a technically demanding task for a variety of reasons, e.g., the presence of 3d electrons, the highly localized wave functions of the oxygen atoms, and the challenge of properly specifying the spin states of the iron atoms. Some theoretical studies of hematite (α-Fe_2O_3) can be found in the literature. There are studies of the surface of hematite that use empirical potentials.[20,21] Using ab initio techniques (primarily plane-wave-based DFT methods), there are several studies of the bulk electronic structure with periodic boundary conditions[22,23,24] and a study of the reconstruction of the surface, also using a periodic wave function approach.[7] Cluster-type simulations have been performed with very small clusters, with a focus on the electronic structure of the bulk crystal;[25] in this work no treatment of the surface was attempted. We used the point-charge technique described in the previous sections to study of the basal surface (001) of hematite (α-Fe_2O_3).

3.1. Computational Methods. All the calculations were carried out with the Jaguar v4.1[26] suite of ab initio quantum chemistry programs on the SP2 parallel supercomputer at PNNL. The ab initio electronic structure of the quantum region was calculated using density functional theory (DFT). In all the calculations, the B3LYP functional[27] was used. As a basis set for the iron atoms, we used for most calculations the Los Alamos LACVP with an effective core potential.[28,29,30] For the oxygen atoms the 6-31G[31] basis set was used. The results from this basis set were tested, as will be discussed below, against larger basis sets, cc-pVTZ(-f)[32] for the oxygen atoms and LACV3P for the iron atoms. The pseudospectral methods in Jaguar,[26] in combination with specialized initial guess algorithms which allow efficient convergence of transition metal containing systems, permitted us to study clusters of considerably large sizes than have typically been employed in the investigation of transition metal oxide clusters. To validate the energetic accuracy of our results, we compared the pseudospectral calculations with fully analytical calculations using Jaguar and also with calculations using the NWChem program[33] for small clusters. These results agreed to within 2 meV, a level of precision which is more than adequate for our purposes.

To apply the algorithm described in Section 2, each cluster of atoms was surrounded by point charges, and point charges were placed at the crystallographic lattice sites. Region 0 was defined as the smallest extended unit cell that could contain the whole cluster of quantum atoms. In the direction perpendicular to the surface, a slab of 15 Å was included in region 0 that leaves a cell with 358 atomic positions. Region 1 was defined as all the point charges within 6 Å, R_1, of any atom in the quantum region. The far region, region 2, included all the point charges between 6 and 12 Å from the quantum atoms. The radius of the embedding region, 12 Å, R_2, and the border between region 1 and region 2 were optimized for the best fitting of the electrostatic potential. Use of a radius larger than 12 Å did not improve the fit appreciably. We used least-squares fitting

with singular value decomposition to remove unstable modes in the charge fitting protocol. The procedure is described in detail in ref 34. The cutoff in the lower eigenvalues was set to 10^{-5} of the largest eigenvalue. This yielded fits with a standard deviation of 0.01 eV/Å. Imposing lower cutoffs did not yield to appreciably better fits of the electrostatic potential, while in some cases it caused unphysically large values of charges to be produced. This problem was not observed using the 10^{-5} cutoff specified above.

In step iii, the electrostatic potential was calculated on a cubic mesh of 0.2 Å on the side. The points of the mesh that were closer than 1.6 Å from one of the quantum centers were discarded. The sampling points were distributed in the bulk of the cluster and above the surface, up to 2.5 Å over the top layer of atoms, resulting in sampling points on the order of 3000. The charges in region 0 were fitted to the electrostatic potential (step iv), constraining the total charge of the cluster and the total charge of the unit cell to be zero. To impose the infinite periodicity of the crystal, for the potential of each point charge, we used the 2-D expression for the potential of a periodic array of point charges[17]

$$U_i(\vec{r}) = \frac{4}{f}\sum_{m=1}^{\infty}\cos(2\pi m\Delta y_i)\sum_{l=-\infty}^{\infty}K_0\left(2\pi\frac{m}{f}[(\Delta x_i l)+\Delta z_i]^{1/2}\right) - \frac{1}{f}\log[\cosh(2\pi\Delta z_i)-\cos(2\pi\Delta x_i)] + C \quad (5)$$

where q_i is one of the point charges in a unit cell, located at position $r_i = (x_i, y_i, z_i)$, f is the ratio of the dimensions of the cell in the directions perpendicular to the surface ($f = L_y/L_x$), the distances are measured in units of L_x, $\Delta\vec{r}_i = (\vec{r}_i - \vec{r})/L_x$, and K_0 is a Bessel function. The constant C is

$$C = -\frac{8}{f}\sum_{l=1}^{\infty}\sum_{m=1}^{\infty}K_0\left(2\pi\frac{lm}{f}\right) - \frac{1}{f}\log\frac{1}{8\pi^2 f^2} - \frac{2\gamma}{f} \quad (6)$$

and $\gamma = 0.5772$.

In step v, we used the charges fitted for the unit cell to calculate the crystal electrostatic potential in the region of the cluster as well as in region 1. Around each lattice site of these two regions, we sampled eight points, chosen at random, at distances between 1 and 1.5 Å from the lattice sites. The effect of sampling more than one point around each lattice site is to incorporate into the fit not only information about the value of the potential at that atom but also with information about the variation of this potential function, i.e., the electric field. The electrostatic potential was calculated at those points using eq 5.

The contribution to the potential energy from the charges inside region 1 was subtracted, leaving us with only the far field. This field was fitted with the charges in region 2 by singular value decomposition. The new charges were used in the following iteration of the algorithm.

3.2. Structural Features of the Model Cluster. The crystal structure of hematite is a corundum structure.[35] In the direction perpendicular to the basal plane (001), layers of closely packed oxygen atoms alternate with two $^1/_3$ layers of iron atoms (bilayers). In the bulk, the distance between oxygen and iron layers is 0.844 Å and between two iron layers is 0.603 Å. The iron atoms make six bonds with oxygen atoms, three long ones, 2.12 Å, and three short ones, 1.94 Å. As for the electronic structure of the bulk, the minimum-energy spin state of the iron atoms is an antiferromagnetic arrangement, where all the iron atoms in a bilayer are arranged parallel and opposite to the spins of the Fe atoms in the next bilayer[22,23] (see Figure 1).

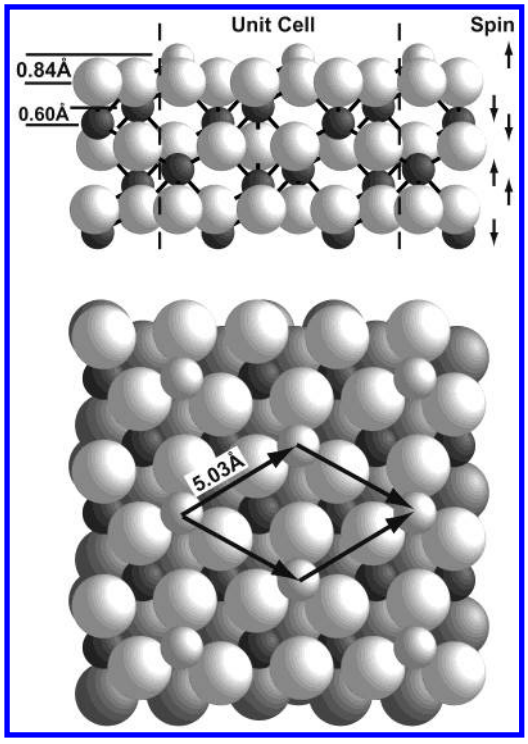

Figure 1. Unit cell of hematite (α-Fe_2O_3) showing the bulk termination. The surface exposed is the iron terminated basal face (001) where the smaller spheres represent iron. For the simulations of the open surface, the interlayer distances were relaxed to the relaxations obtained by ref 7. The spin of the iron atoms is antiferromagnetic where atoms in the two layers between two oxygen layers have parallel spin and are opposite to the spin of the atoms on the next bilayer.

When cleaved, the (001) surface of hematite is terminated by a $^1/_3$ layer of iron atoms. The layers closest to the surface relax inward by a significant amount, as shown by classical[21] and ab initio simulations.[7] The latter calculation refers to a periodic DFT simulation of the reconstruction at the surface using a slab configuration. The interlayer distances were found to relax by −57%, 7%, −33%, 15%, 5%, −3%, 1%, and 4%, starting with the top $Fe-O_3$ interlayer separation and proceeding downward. We used these interlayer distances for the surface structure of the cluster.

One important task in the cluster simulation of crystals is the picking of the right size of the cluster. As in any computer simulation, the cluster has to be as small as possible to minimize computational efforts, but it also has to be large enough to mimic well the properties of the system under study. If the crystal were perfectly ionic, that is, a lattice of point charges, then any size of cluster would be a perfect representation. As the crystal deviates from the ionic model, larger clusters are necessary, until the "rest of the crystal" is far away enough to make the point charge representation an acceptable one. To find the right cluster size for our simulations, we had to systematically increase the size of the cluster, in both surface area and in depth. The successive clusters were chosen to maintain the correct stoichiometry of hematite and to maintain the antiferromagnetic spin state with a total spin 0 state. The clusters were cut from a crystal with a reconstructed surface, as mentioned above. The clusters satisfying these two requirements are of prismatic shape (see Figure 2).

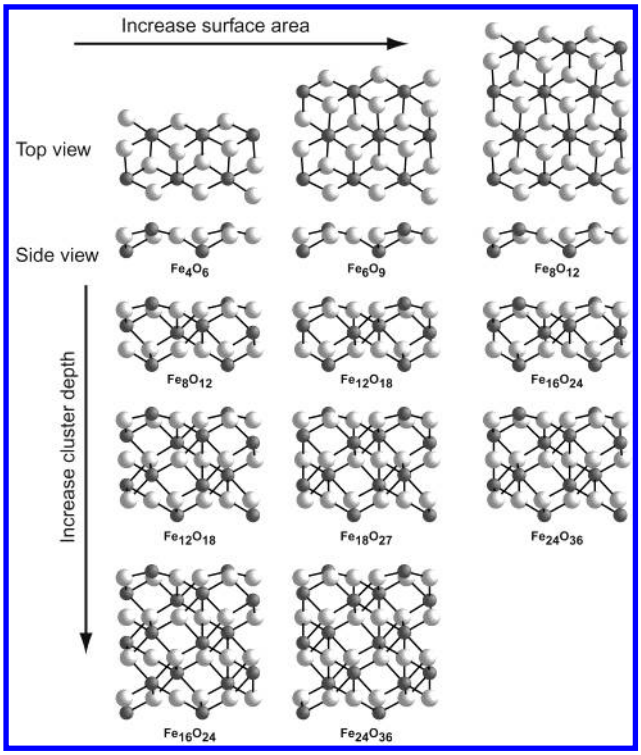

Figure 2. Hematite clusters used for the study of convergence of cluster behavior to bulk. The clusters are prismatic in shape. The surface area of the cluster increases on the horizontal axis, while in the vertical axis the depth of the cluster grows.

In the next section, we present the clusters studied, the properties calculated, and the study of the approach to the bulk behavior.

4. Results

To study the convergence of the cluster to the bulk behavior, we studied clusters of increasing sizes. The clusters studied are shown in Figure 2. The clusters studied ranged from a 10-atom cluster (Fe_4O_6) to clusters with 60 atoms ($Fe_{24}O_{36}$). The clusters were systematically enlarged by taking larger and larger areas of the surface (horizontal axis in Figure 2). The clusters were also enlarged in the direction perpendicular to the surface by taking clusters that extended deeper into the bulk of the crystal. The surface area was varied from 44 to 88 Å^2. The depth of the quantum region was increased from 1.5 Å (3 layers of atoms) to 8.14 Å (13 layers of atoms).

The self-consistent loop described in section 2 was applied to calculate the point charges. The loop had to be iterated on the order of 10 times to achieve convergence. When converged, the point charges in the unit cell located at the iron positions vary between 0.9 and 2 au (1 au = 1.6 10^{-19} C), and the charge at the oxygen location is between −0.4 to −1.2 electrons.

To decide how large a cluster has to be to simulate the crystal, one has to decide on a parameter that measures the effect of the point charges on the cluster. The net effect of the embedding method is to model the electrostatic interaction of the cluster with the rest of the crystal. One quantity that is particularly sensitive to the electrostatic potential in the region of the cluster is the ionization energy of the cluster. We used this energy, therefore, as a size parameter to monitor the convergence of the cluster to the bulk behavior. The ionization energy of the cluster was computed as

$$IE = E(N_{e^-} - 1) - E(N_{e^-}) \qquad (7)$$

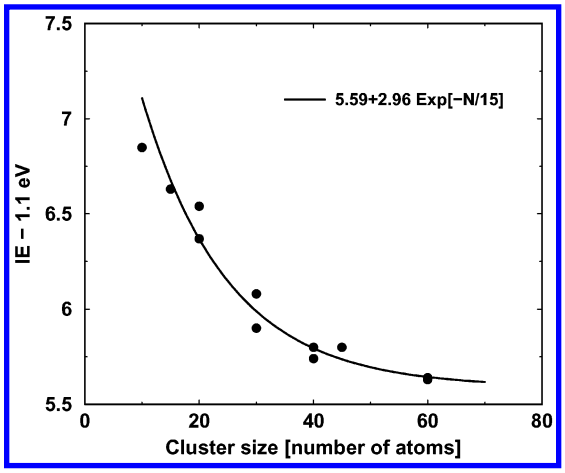

Figure 3. Ionization energy of the cluster as function of the cluster size (total number of atoms in the cluster) and fitting curve. One-half of the experimental band gap of hematite has been subtracted to the ionization energy to show the convergence of these energies to the work function.

where N_{e^-} is the number of electrons in the cluster and E is the total energy of the system. In Figure 3 we present the ionization energy of the cluster as function of the total number of atoms in the cluster. One-half of the experimental band gap of hematite ($\Delta E^{(exp)}_{Fe_2O_3}$ = 2.2 eV[36]) was subtracted from the ionization energy of the clusters so that it would yield the work function, $\Phi = IE - 1.1$ eV, in the bulk limit. The energy points were fitted with an exponential function as a function of the total number of atoms in the cluster, $N = N_{Fe} + N_O$, as follows:

$$\Phi_{Fe_2O_3(001)} = 5.59 \text{ eV} + 2.96e^{-N/15} \text{ eV} \qquad (8)$$

In the limit of large N, eq 8 gives the value of the work function for the (001) basal plane of hematite, $\Phi_{Fe_2O_3(001)} = 5.59$ eV.

Several tests were run using a 30 atom cluster $Fe_{12}O_{18}$ to investigate the sensitivity of these results to various aspects of the calculations. When the basis set is enlarged using LACV3P for the iron atoms and cc-VTZ(-f) oxygen atoms, the change in ionization energy is 0.15 eV, that is, a difference of 2%. Using a different DFT functional, PW91,[5,6] caused an ionization energy change of 0.2 eV. The effect of the embedding charges was tested by calculating the work function in one of our largest clusters, $Fe_{24}O_{36}$, with and without the embedding charges. We found a difference of 0.6 eV, that is, a change of 10% between the energy of the embedded cluster and the energy of a bare cluster (no charges around). Using formal charges at the ion sites, 3 au at the iron atoms and −2 au at the oxygen sites, we obtain a much smaller work function, 4.08 eV for a 30-atom cluster, 1.91 eV lower than the energy in Figure 3.

Some experimental data are available for comparison with our calculations. Measurements of electrical properties of hematite in different conditions of vacuum and at various temperatures have been reported by Glitzer et al.[37] The experimental measurements of the work function of hematite were reported relative to the work function of their platinum tip, revealing the hematite work function to be lower by approximately 0.3 eV in the limit of high vacuum and for their lowest experimental temperatures. The work function for platinum varies between 5.12 and 5.93 eV, and it is 5.64 eV for the polycrystalline system.[38] This places our calculation within the range of energies expected from the experimental observations. Measurements of work functions in different types or iron oxides have been reported by Ranke and Weiss.[39] This

experimental work found the work function of the (111) face of wustite, FeO, to be $\Phi_{FeO(111)} = 5.90$ eV, and for the (111) face of magnetite, Fe_3O_4, the measured work function is $\Phi_{Fe_3O_4(111)} = 5.52$ eV. Even though these are not the same types of iron oxide surface as the one used in our calculations, the results again suggest that our calculations are in the right range as compared to the experiment. While there is still some discussion on whether wustite is oxygen-terminated or iron-terminated, the (111) surface of magnetite bears some resemblance to the (001) surface of hematite. Along the direction normal to the surface, magnetite also alternates layers of closed packed oxygen with layers of iron. The surface layer of magnetite is formed by a $^1/_4$ layer of iron atoms on top of a hexagonal closely packed layer of oxygen atoms. The iron atoms, as compared to those on the surface of hematite, form a hexagonal lattice with an iron−iron separation of 5.92 Å for magnetite versus 5.04 Å on the surface of hematite. We find that our calculated work function for hematite matches well with the range of experimental values for the other two oxides[39] as well as with the measurements by Glitzer et al.[37]

5. Discussion

We have presented an algorithm to calculate the point charges required to surround a cluster of quantum atoms to generate a crystal environment. This algorithm can be applied to generate the crystal field for simulations of surface phenomena. The importance of such a method is that with it one can study the local chemistry and physics of crystals, such as chemical reactions or crystal defects. One could also carry out geometry optimizations using the present methodology. For a bare, neutral surface, it is not clear how this would compare (in terms of CPU time or accuracy) with plane wave approaches. We intend to implement this capability in future work.

The limitations of this method come from the starting assumption that the rest of the crystal can be modeled as a lattice of point charges. The more covalent the crystal is, the farther away the point-charge-modeled atoms will have to be for the model to be applicable. This will force one to work with large clusters.

The application of the point charges plus quantum cluster algorithm to the study of the basal surface of hematite shows that the required point charges are considerably smaller than the formal charges of the atoms. We also found that to converge the size of the cluster to achieve crystal behavior on the removal of one electron, the cluster has to be on the order of 60 atoms. This is a rather strict test for a cluster simulation. In other types of simulations, where the change in the electronic structure is more localized, as in the case of a binding of a molecule to the surface, one might be able to work with smaller clusters.

From the study of hematite we were able to calculate the value of the work function of the basal face, $\Phi_{Fe_2O_3(001)} = 5.6$ eV. This calculated value matches well with the range expected from experimental studies of electric properties of hematite as well as experiments performed on cousin iron oxide structures, magnetite, and wustite.

Acknowledgment. This work was supported by the National Science Foundation and the Department of Energy under Grant No. 9810367 for the Environmental Molecular Sciences Institute at Columbia University.

References and Notes

(1) Car, R.; Parrinello, M. *Phys. Rev. Lett.* **1985**, *55*, 2471.
(2) Vienna ab Initio Simulation Package (VASP). http://cms.mpi.univie.ac.at/vasp.
(3) Troullier, N.; Martins, J. *Phys. Rev. B* **1991**, *43*, 1993.
(4) Kresse, G.; Hafner, J. *J. Phys.: Condens. Matt.* **1994**, *6*, 8245.
(5) Perdew, J. In *Electronic Structure of Solids '9*; Ziesche, P., Schrig, H., Eds.; Akademie Verlag: Berlin, 1991; p 11.
(6) Perdew, J. P.; Wang, Y. *Phys. Rev. B* **1992**, *45*, 13244.
(7) Wang, X.-G.; Weiss, W.; Shaikhutdinov, S.; Ritter, M.; Petersen, M.; Wagner, F.; Schlögl, R.; Scheffler, M. *Phys. Rev. Lett.* **1998**, *81*, 1038.
(8) Ewald, P. *Ann. Phys. (Leipzig)* **1921**, *64*, 253.
(9) de Leeuw, S.; Perram, J.; Smith, E. *Proc. R. Soc. London, Ser. A* **1980**, *373*, 27.
(10) Stefanovich E.; Truong T. *J. Phys. Chem. B* **1998**, *102*, 3018.
(11) Sousa C.; Casanovas J.; Rubio J.; Illas F. *J. Comput. Chem.* **1993**, *14*, 680.
(12) Derenzo, S.; Klintenberg, M.; Weber, M. *J. Chem. Phys.* **2000**, *112*, 2074.
(13) Allen, M.; Tildesley, D. *Computer Simulation of Liquids*; Oxford University Press: New York, 1987.
(14) Stefanovich, E.; Truong, T. *Chem. Phys. Lett.* **1999**, *299*, 623.
(15) Rittner, F.; Fink, R.; Boddenberg, B.; Staemmler, V. *Phys. Rev. B* **1999**, *57*, 4160.
(16) Lekner, J. *Phy. A* **1991**, *176*, 485.
(17) Clark, A.; Madden, T.; Warren, P. *Mol. Phys.* **1996**, *87*, 1063.
(18) Kung, H. *Transition Metal Oxides: Surface Chemistry and Catalysis*; Elsevier: Amsterdam, 1989; Vol. 45.
(19) Kordas, G.; Weeks, R.; Arfsten, N. *J. App. Phys.* **1985**, *57*, 3812.
(20) Mackrodt, W.; Davey, R.; Black, S. *J. Cryst. Growth* **1987**, *80*, 441.
(21) Wasserman, E.; Rustad, J.; Felmy, A.; Halley, J. *Surf. Sci.* **1997**, *385*, 217.
(22) Sandratskii, L.; Kübler, J. *Europhys. Lett.* **1996**, *33*, 447.
(23) Sandratskii, L.; Uhl, M.; Kübler, J. *J. Phys.: Condens. Matter* **1996**, *8*, 983.
(24) Catti, M.; Valerio, G.; Dovesi, R. *Phys. Rev. B* **1995**, *51*, 7441.
(25) Armelao, L.; Bettinelli, M.; Casarin, M.; Granozzi, B.; Tondello, E.; Vittadini, A. *J. Phys.: Condens. Matter* **1995**, *7*, L299.
(26) *Jaguar v. 4.1*. Schrodinger, Inc.: Portland, OR, 2000.
(27) Becke, A. *J. Chem. Phys.* **1993**, *98*, 1372.
(28) Hay, P.; Wadt, W. *J. Chem. Phys.* **1985**, *82*, 270.
(29) Hay, P.; Wadt, W. *J. Chem. Phys.* **1985**, *82*, 299.
(30) Wadt, W.; Hay, P. *J. Chem. Phys.* **1985**, *82*, 284.
(31) Hehre, W.; Ditchfield, R.; Pople, J. *J. Chem. Phys.* **1972**, *56*, 2257.
(32) Jr., T. D. *J. Chem. Phys.* **1989**, *90*, 1007.
(33) Anchell, J.; Apra, E.; Bernholdt, D.; Borowski, P.; Bylaska, E.; Clark, T.; Clerc, D.; Dachsel, H.; de Jong, W.; Deegan, M.; Dupuis, M.; Dyall, K.; Elwood, D.; Fann, G.; Fruchtl, H.; Glendenning, E.; Gutowski, M.; Harrison, R.; Hess, A.; Jaffe, J.; Johnson, B.; Ju, J.; Kendall, R.; Kobayashi, R.; Kutteh, R.; Lin, Z.; Littlefield, R.; Long, X.; Meng, B.; Nichols, J.; Nieplocha, J.; Rendall, A.; Rosing; Sandrone, G. M.; Stave, M.; Straatsma, T.; Taylor, H.; Thomas, G.; van Lenthe, J.; Windus, T.; Wolinski, K.; Wong, A.; Zhang, Z. *NWChem, a Computational Chemistry Package for Parallel Computers*, Version 3.3.1; Pacific Northwest National Laboratory: Richland, WA, 1999.
(34) Press, W.; Flannery, B.; Teukolsky, S.; Vetterling, W. *Numerical Recipes*; Cambridge University Press: Cambridge, 1989; Section 2.9.
(35) Finger, L. *J. App. Phys.* **1980**, *51*, 5362.
(36) Sanchez, C.; Hendewerk, M.; Sieber, K.; Somarjai, G. *J. Solid State Chem.* **1986**, *61*, 47.
(37) Gleitzer, C.; Nowotny, J.; Rekas, M. *Appl. Phys. A* **1991**, *53*, 310.
(38) *CRC Handbook of Physics and Chemistry*; CRC Press: Boca Raton, FL 1996.
(39) Ranke, W.; Weiss, W. *Surf. Sci.* **1998**, *414*, 236.